ACS Macro Letters

Letter

pubs.acs.org/macroletters

Achieving Bicontinuous Microemulsion Like Morphologies in Organic Photovoltaics

Dylan Kipp,[†] Olga Wodo,[‡] Baskar Ganapathysubramanian,[§,∥] and Venkat Ganesan*[,†]

[†]Department of Chemical Engineering, University of Texas at Austin, Austin, Texas 78712, United States

[‡]Mechanical and Aerospace Engineering Department, University of Buffalo, Buffalo, New York 14260, United States

[§]Department of Mechanical Engineering and [∥]Department of Electrical and Computer Engineering, Iowa State University, Ames, Iowa 50011, United States

Supporting Information

ABSTRACT: It is believed that the optimal morphology of an organic solar cell may be characterized by cocontinuous, interpenetrating donor and acceptor domains with nanoscale dimensions and high interfacial areas. One well-known equilibrium morphology that fits these characteristics is the bicontinuous microemulsion achieved by the addition of block copolymer compatibilizers to flexible polymer−polymer blends. However, there does not exist design rules for using block copolymer compatibilizers to produce bicontinuous microemulsion morphologies from the conjugated polymer/fullerene mixtures typically used to form the active layer of organic solar cells. Motivated by these considerations, we use single chain in mean field simulations to study the equilibrium phase behavior of semiflexible polymer + flexible−semiflexible block copolymer + solvent mixtures. Based on our results, we identify design rules for producing large channels of morphologies with characteristics like that of the bicontinuous microemulsion.

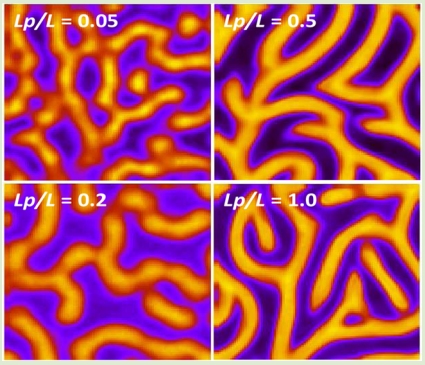

The device performance of organic solar cells (OSCs) has been speculated to sensitively depend on the active layer morphology.[2,3] Specifically, it is believed that the optimal active layer morphology may be characterized by cocontinuous, interpenerating donor and acceptor domains with nanoscale dimensions and high interfacial areas. Bicontinuous microemulsions (BμE),[4−9,16] which are equilibrium morphologies achieved by the addition of block copolymer (BCP) compatibilizers to flexible polymer blends, are known to possesses such characteristics. In comparison to lamellar morphologies, BμE morphologies may be preferable for OSC applications since they percolate in all three directions. Hence, active layers based on the BμE morphology may provide continuous pathways for the electrons and holes to travel to the electrodes, regardless of the orientation of the domains immediately neighboring the electrodes. Moreover, since BμE morphologies are characterized by a broader distribution of domain sizes than are lamellar morphologies, the design of efficient OSCs based on the BμE morphology may depend less on the targeting of a single "ideal" domain size.

Unfortunately, the kinds of flexible polymeric materials that have been noted to form BμEs are typically not appropriate for use in OSC active layers. Rather, high efficiency OSCs are often based on a blend of photoactive, electron-donating, conjugated polymers and electron-accepting, fullerene molecules. Within such a framework, an outstanding question is whether block copolymer compatibilizers can be used to achieve BμE morphologies also in the case of conjugated polymer/fullerene blends. More specifically:

1. The spherical fullerene molecule is much smaller in size than the conjugated polymer donor and is more appropriately viewed as a solvent particle relative to the size of the polymer segments.[10,11] This motivates the first question we consider: Can BCP compatibilizers be used to produce BμE morphologies in the case of polymer/solvent blends?
2. The conjugated donor polymer is characterized by a natural degree of rigidity and is, in many instances, subject to either liquid crystalline ordering or polymer crystallization: either effect is expected to have a strong influence on the morphology.[3] This raises the second question we consider: Do the polymer/solvent BμE morphologies, if they exist at all, persist for the case of nonflexible donor polymer materials?

In the case of flexible polymer blends, experiments have typically identified the channel of bicontinuous microemulsion in the vicinity of the Lifshitz point (i.e., the intersection of the critical Scott line and the microphase-to-macrophase transition line, see Figure 1).[4,5] Fluctuations promote competition between microphase and macrophase separation around this region, thus, disrupting the lamellar phase and producing the channel of BμE. For two equal molecular weight homopolymers A and B and a block copolymer (BCP) AB, the Scott line

Received: January 2, 2015
Accepted: February 4, 2015
Published: February 5, 2015

DOI: 10.1021/acsmacrolett.5b00007
ACS Macro Lett. 2015, 4, 266−270

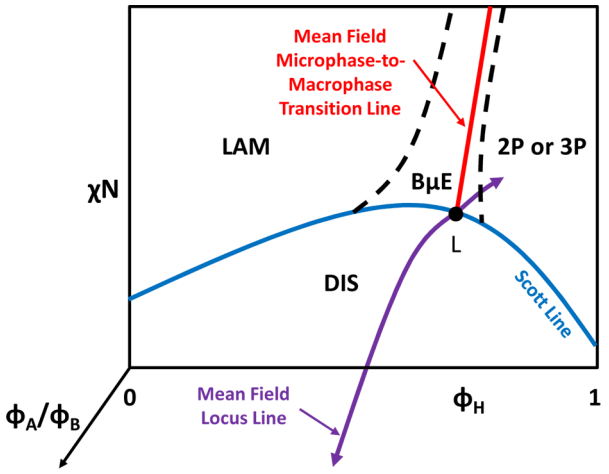

Figure 1. Schematic of phase behavior for a ternary blend system of homopolymers A and B with a diblock copolymer AB. $\phi_H = \phi_A + \phi_B$ is the total homopolymer volume fraction and the strength of compositional interactions is measured by the Flory–Huggins parameter, χ. The regions labeled LAM, DIS, and 2P or 3P are regions of thermodynamically stable lamellar, disordered, and 2-phase or 3-phase coexistence, respectively. The thermally induced channel of BμE forms due to fluctuations at the Lifshitz point (L, i.e., the intersection of the mean field microphase-to-macrophase transition line and the Scott line). The Scott line is a special instance of the mean field spinodal line that results for a specified ratio ϕ_A/ϕ_B. By varying ϕ_A/ϕ_B, a mean field microphase-to-macrophase transition plane and spinodal plane form. The intersection of these two planes form a line that we refer to as the mean field locus line. This schematic was adapted from Fredrickson and Bates.[5]

is located on the isopleth $\phi_A = \phi_B = 1 - 2\phi_{AB}$ (where ϕ_i is the blend volume fraction of material i). However, in the case of blends of components with unequal molecular weights, the Scott line composition is determined by the relationship $\alpha_A\phi_A^2 = \alpha_B\phi_B^2$ (where α_i is the ratio of the degree of polymerization of the polymer i over the degree of polymerization of the BCP).[5] Such a relationship suggests that the ratio of the donor and acceptor volume fractions corresponding to the Scott line is likely to be very small for polymer/solvent mixtures. On the other hand, high efficiency organic solar cells are typically based on symmetric or near-symmetric donor/acceptor blend ratios.[3] Hence, active layers based on polymer/solvent ratios corresponding to the Scott line are likely to yield suboptimal device efficiencies, even if they are characterized by cocontinuous donor and acceptor domains.

The conflict described above motivates the search for BμE morphologies over a wider range of polymer/solvent ratios (closer to the conditions known to yield better device properties and away from the Scott line). We note that, by varying the polymer/solvent blend ratio, the mean field microphase-to-macrophase transition line and the spinodal line (of which the Scott line is a special instance) become planes in full ternary composition space. The intersection of these two planes forms a line that we refer to in this Letter as the "mean field locus line." Since the formation of BμE morphologies depends on the competition between microphase and macrophase separation that takes place at the mean field microphase-to-macrophase transition, and considering that there is no guarantee that the microphase morphology to the high BCP side of a mean field microphase-to-macrophase transition will be characterized by cocontinuous donor and acceptor domains, *we hypothesize that polymer/solvent BμE*

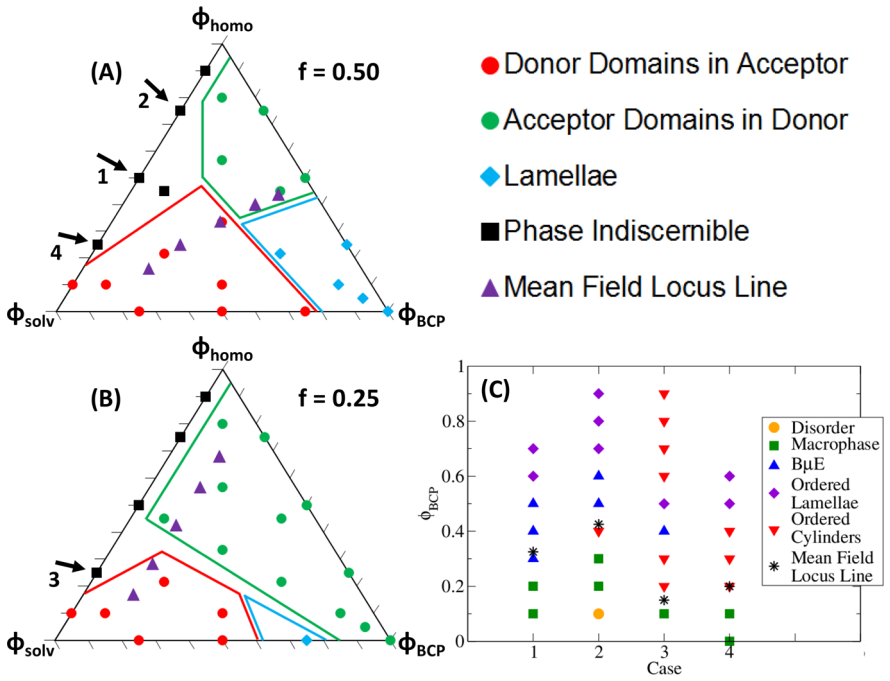

Figure 2. Phase diagrams for polymer/BCP/solvent blend system in case of all flexible polymer materials ($L_p/L = 0.05$). Panels A and B plot the ternary phase diagrams for $f = 0.5$ and $f = 0.25$ with $\chi N = 50$ for both cases. These two diagrams were adapted from Kipp and Ganesan.[22] The solid lines approximately partition the diagram into different phases. We searched for BμEs along the trajectories indicated by the four arrows in Panels A and B. Panel C is the location of the BμE channels for the cases indicated by the four arrows and at values of χN just above the $\chi N_{spinodal}$: (1) $f = 0.5$, $\phi_{homo}/\phi_{solv} = 1$, $\chi N = 20$; (2) $f = 0.5$, $\phi_{homo}/\phi_{solv} = 3$, $\chi N = 16$; (3) $f = 0.25$, $\phi_{homo}/\phi_{solv} = 1/3$, $\chi N = 29$; (4) $f = 0.5$, $\phi_{homo}/\phi_{solv} = 1/3$, $\chi N = 24$. In Panel C, $\phi_{BCP} = 1 - \phi_{homo} - \phi_{solv}$.

DOI: 10.1021/acsmacrolett.5b00007
ACS Macro Lett. 2015, 4, 266–270

morphologies may form even away from the Scott line at points along the mean field locus line that correspond to a transition to the lamellar phase.

To validate the above hypothesis, we study the phase behavior of a model for the conjugated polymer/BCP/fullerene blend system. As a simple coarse-grained representation for such a system, we consider a mixture of semiflexible homopolymer B, flexible−semiflexible block copolymer AB, and explicit solvent S. We use five parameters to characterize the components of our model: (i) f denotes the volume fraction of the flexible A block of the BCP, (ii) L_p/L denotes the ratio of the persistence length of the semiflexible B components (i.e., the homopolymer and B block of the BCP) normalized by the length of the BCP (the cases of L_p/L = 0.05 and L_p/L = 1.0 represent the limiting cases of fully flexible and nearly rod-like chains, respectively), (iii) χ_{ij} denotes the strength of Flory−Huggins interactions between components i and j, (iv) μ denotes the strength of Maier−Saupe interactions between the semiflexible B components used to capture the liquid crystalline nature of the donor materials, and (v) N denotes the degree of polymerization of both the BCP and the homopolymer. We choose to set the various interactions parameters (χ_{ij} and μ) such that they are in proportion to a parameter χ, which we vary in order to explore different areas of the phase space. We select these proportions such that $\chi_{AS} < \chi_{AB} = \chi_{BS}$ in order to place the BCP at the interface of the homopolymer and solvent, thus, making the BCP a compatibilizer. Further details of the choice of the parameters are relegated to the Supporting Information.

The BμE phases are inherently fluctuation driven, and hence are not amenable to study by mean-field theories. In our previous work, we demonstrated that the methodology of single chain in mean field (SCMF)[1,13−17] simulations enables the identification of such morphologies and furnishes phase boundaries that are in accord with more sophisticated approaches.[16,17] Moreover, although the BμE is fundamentally a three-dimensional morphology, previous studies of BμE phases have demonstrated qualitative agreement between the results of two-dimensional (2D) simulations and experimental observations.[9,16] Inspired by these successes, in this work, we use the SCMF approach with two-dimensional variation of the composition and orientation order parameter fields (although the positions of the monomers are evolved in three dimensions) as the main tool to study the phase behavior of our model and to identify the channels of BμE morphologies.

We first test the validity of our hypothesis regarding the formation of polymer/solvent BμEs in the context where both the A block of the BCP and the donor B components are treated as flexible polymer chains. We use the random phase approximation (RPA)[12] to calculate the mean field locus lines and the SCMF method to generate very coarsely sampled ternary phase diagrams for a collection of polymer/BCP/solvent combinations (see Figure 2A,B). Although the phases indicated in Figure 2A,B are for a value of $\chi N \gg \chi N_{spinodal}$, we observe that the compositional phase lines move only slightly with increasing χN. Hence, we compare the compositions of the mean field locus lines and of the various phase transitions in these figures to identify the expected location of the channels of BμE.

In Figure 2A,B, we observe that the majority of each mean field locus line lies within the phase space of either donor-rich or acceptor-rich domains suspended in the continuous opposite domain. Therefore, the transition from macrophase to microphase separation for these blend formulations does not represent a transition to a BμE morphology, but rather a transition to a morphology in which only the donor or only the acceptor forms continuous domains. We also observe that both (1) the entirety of the apparent lamellar phase transition line in the case of f = 0.25 (Figure 2B) and (2) the portion of the lamellar phase transition line corresponding to $\phi_{homo}/\phi_{solv} <$ 0.5 in the case of f = 0.5 (Figure 2A) do not lie near the mean field locus lines. Based on our hypothesis above, we expect that such regions of the phase diagram are not likely to yield BμE morphologies. Interestingly, however, in the case of f = 0.5 and $\phi_{homo}/\phi_{solv} \geq$ 0.5 (Figure 2A), the mean field locus line closely coincides with the apparent transition from acceptor-rich domains suspended in donor to a lamellar morphology. Accordingly, we hypothesized that these blend formulations would be the most likely to form BμEs. To test the validity of our predictions, we examined select areas of the phase space in the proximity of the $\chi N_{spinodal}$ in greater detail. Explicitly, the arrows in Figure 2A,B indicate such regions of the phase space we examined for evidence of BμE morphologies.

Figure 2C summarizes the results from our search for BμE morphologies in the case of all flexible polymer chains. We observe that the largest envelope of bicontinuous microemulsion results in the case of f = 0.5, ϕ_{homo}/ϕ_{solv} = 1, and χN = 20 (Figure 2C, case 1). For this case, the macrophase-to-microphase transition with increasing ϕ_{BCP} indeed corresponds to a transition from a macrophase-separated morphology to a microphase-separated BμE morphology. Accordingly, the corresponding point of the mean field locus line (see Figure 2A,C, case 1) represents a direct transition to BμE morphologies. Our hypothesis would suggest the formation of a large channel of BμE for these conditions, which is validated by the observed results.

In each of the other cases (Figure 2C, cases 2−4), we observe a transition from a macrophase-separated morphology to an ordered cylinder morphology with increasing ϕ_{BCP}. A channel of BμE is still evident (except in case 4), but the onset of the channel of BμE (ϕ_{BCP}^{crit}) is seen to have shifted to a higher ϕ_{BCP}. As the channel of ordered cylinders preceding the BμE expands, the channel of BμE thins. In case 4 of Figure 2C, the channel of ordered cylinders is its widest, and the channel of BμE collapses to zero.

We recall that, in cases 2−4 (and especially in cases 3 and 4), the lamellar phase transition line is not close to the mean field locus line in our ternary phase diagrams (Figure 2A,B). Hence, our hypothesis would suggest that such conditions are less likely to yield BμE morphologies. Indeed, we observe that the largest channel of BμE results in the case where the lamellar phase transition line coincides with the mean field locus line (case 1). As the lamellar transition moves away from the mean field microphase-to-macrophase transition (cases 2−4), the impetus for macrophase separation in the vicinity of the channel of BμE weakens, and hence, the channel of BμE thins. Overall, the results presented in Figure 2 confirm that the formation of BμEs depends on the overlap of the mean field locus line and the onset of microphase-separated lamellar phases. In a longer version of this letter, we will present results for other parametric conditions that serve to substantiate these conclusions. In response to the first of the questions raised in the introduction, the above results together suggest that indeed block copolymer compatibilizers may be used to achieve BμE morphologies and that such morphologies can be achieved even

DOI: 10.1021/acsmacrolett.5b00007
ACS Macro Lett. 2015, 4, 266−270

away from the Scott line and closer to the experimentally relevant conditions.

Now we present our results for the case where the donor B chains are characterized by a finite persistence length. Explicitly, Figure 3A displays the results for the case of $\phi_{homo}/\phi_{solv} = 1.0$,

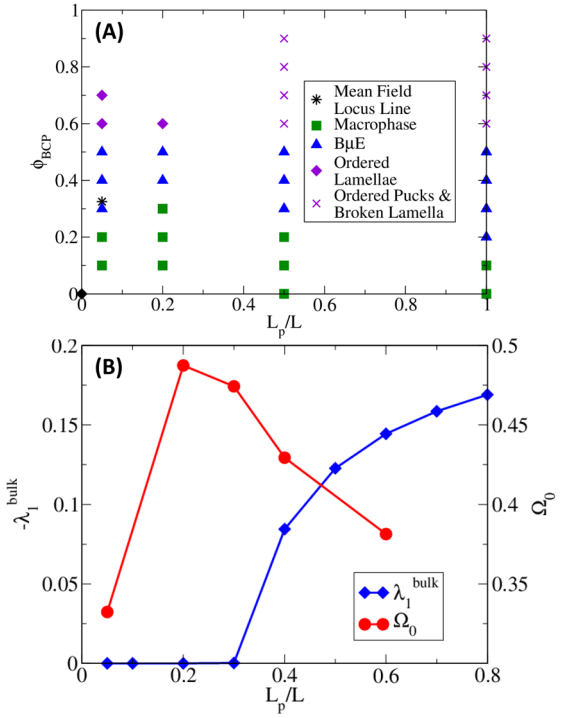

Figure 3. Phase behavior and interfacial characteristics of a polymer/BCP/solvent blend system in case of a semiflexible donor polymer. For all cases, $\phi_{homo}/\phi_{solv} = 1$, $f = 0.5$, and $\phi_{BCP} = 1 - \phi_{homo} - \phi_{solv}$. Panel A plots the phase behavior resulting from the SCMF simulations in the case of $\mu = 4\chi$. For these simulations, we reduce χN as we increase L_p/L in order to remain near to the compositional order−disorder transition. Panel B plots the interfacial characteristics resulting from 1D SCFT calculations in the case of $\chi N = 26$ and $\mu = 2\chi$.

and $f = 0.5$, for increasing L_p/L. We observe that the BμE morphologies that form in the case of flexible ($L_p/L = 0.05$) polymers also persist in the case of semiflexible ($L_p/L > 0.05$) donor chains. In the Supporting Information, we present some pictorial evidence (see Figure S1) to demonstrate that the morphologies resulting for different L_p/L do resemble the characteristics observed in the better known case of flexible polymer/polymer systems. Moreover, we also characterize the morphologies by a variety of measures to probe whether they possess the features discussed in the introduction as being desirable for OPV applications (e.g., a distribution of donor and acceptor domain sizes). Together, these results address the second question raised in the introduction and confirm that BμE-like morphologies do persist even when the donor polymer possesses a finite persistence length.

Interestingly, in Figure 3A, we observe that the location and width of the channel of BμE sensitively depends on L_p/L. For instance, increasing the donor chain rigidity from $L_p/L = 0.05$ to $L_p/L = 0.2$ is seen to result in an increased ϕ_{BCP}^{crit} and a thinner channel of BμE, but that further increasing the donor chain rigidity from $L_p/L = 0.2$ to $L_p/L = 0.5$ and from $L_p/L = 0.5$ to $L_p/L = 1.0$ results in a decreased ϕ_{BCP}^{crit} and an expanded channel of BμE. Indeed, the smallest ϕ_{BCP}^{crit} and the largest channel of BμE results in the case of highly rigid donor chains.

We note that, in the case of flexible ternary polymer blends, the formation of microemulsion morphologies has typically been associated with ultralow interfacial tensions induced by the BCP on the polymer blend.[23] Motivated by these results, we consider the interfacial tension for our polymer/BCP/solvent blend as a means to understand the intriguing and nonmonotonic influence of the persistence length noted in Figure 3A. Accordingly, we used the framework of polymer self-consistent field theory (SCFT)[18−21] to calculate the interfacial activity of the BCP in a polymer/solvent blend (the details of the SCFT calculations are provided in the Supporting Information). We present the main result in Figure 3B, wherein we display the influence of the persistence length upon the amount of excess BCP at the interface required to reduce the interfacial tension to zero (denoted in the figure as Ω_0). Starting with flexible ($L_p/L = 0.05$) donor chains, we observe that increasing L_p/L leads to an initial increase in Ω_0. However, further increase of L_p/L beyond a critical value is seen to lead to a decrease in Ω_0. These results are, in-turn, explained by consideration of the orientational order within the system. Explicitly, in Figure 3B we display the primary eigenvalue, λ_1^{bulk}, associated with the orientational order in the donor-rich bulk. We observe that there is a critical chain rigidity, L_p/L^{crit}, above which the donor-rich bulk of the polymer/BCP/solvent blend mixture is orientationally ordered. Moreover, Ω_0 is seen to peak at a value of L_p/L comparable to L_p/L^{crit}.

Taken together, the results of the SCFT calculations presented in Figure 3B indicate that the interfacial activity (or equivalently, the efficacy of the BCP in reducing the interfacial tension) of the BCP decreases (increases) with an increase in L_p/L when the system is orientationally disordered (ordered). We believe that the primary effect in this regard is the dependence of the "bare" (in the absence of BCP compatibilizers) homopolymer−solvent interfacial tension upon L_p/L. Physically, the introduction of an interface between the donor and acceptor domains results in an energetic cost arising from the need for the semiflexible chains to bend and avoid excursions to the unfavorable phase. This energetic penalty is expected to increase with an increase in L_p/L when the system is orientationally disordered. However, in the case of an orientationally ordered donor domain, by choosing the plane of orientational order to correspond to the interfacial plane, such an energy cost is avoided. Hence, an increase in orientational order results in a reduction in the homopolymer−solvent interfacial tension. Not surprisingly, the Ω_0 corresponding to the interfacial activity of the BCP mirrors such a dependence on L_p/L.

In Figure S5 of the Supporting Information, we present evidence that the donor domains of the BμEs observed for the parameters corresponding to Figure 3A are not orientationally ordered in the cases of $L_p/L = 0.05$ and $L_p/L = 0.2$, but that they are orientationally ordered in the cases of $L_p/L = 0.5$ and $L_p/L = 1.0$. These trends serve to explain the observations in the context of the phase behavior depicted in Figure 3A. Explicitly, we would expect ϕ_{BCP}^{crit} (resulting from the SCMF simulations) to behave similar to the trends exhibited by Ω_0. Indeed in Figure 3A, we observe that ϕ_{BCP}^{crit} increases as a result of increasing L_p/L from below the orientational order−disorder transition (where the donor domains are orientationally disordered) and that, subsequent to the orientational ordering

DOI: 10.1021/acsmacrolett.5b00007
ACS Macro Lett. 2015, 4, 266−270

of the donor domains, further increase of L_p/L leads to a decrease in ϕ_{BCP}^{crit}.

To summarize, we presented a theoretical analysis of the ternary phase behavior of semiflexible polymer + flexible-semiflexible BCP + solvent to demonstrate that it may be possible to produce BμE morphologies from conjugated polymer/fullerene blends. Moreover, we identified a simple design rule for such BμE phases by positing their formation to be correlated to points along the mean field locus line that represent a transition to a lamellar morphology. In addressing the semiflexible nature of the conjugated polymer material, we found that BμEs are also formed in cases where the donor polymer has a finite persistence length and that they exhibit characteristics similar to those noted for the flexible polymer systems. Moreover, we identified an intriguing influence of the persistence length of the donor on the interfacial activity of the BCP: increasing L_p/L from the state of an orientationally disordered donor domain results in a decreased interfacial activity of the BCP and a larger amount of BCP required to form microemulsions. However, increasing L_p/L from the state of an orientationally ordered donor domain results in an increased interfacial activity of the BCP and a smaller amount of BCP required to form microemulsions.

■ ASSOCIATED CONTENT

Supporting Information

Model details and quantitative morphological characterization of BμE morphologies. This material is available free of charge via the Internet at http://pubs.acs.org.

■ AUTHOR INFORMATION

Corresponding Author

*E-mail: venkat@che.utexas.edu.

Notes

The authors declare no competing financial interest.

■ ACKNOWLEDGMENTS

This work was supported in part by grants from the Robert A. Welch Foundation (Grant F1599), the National Science Foundation (CBET-1264583), and the U.S. Army Research Office (W911NF-13-1-0396). The authors acknowledge the Texas Advanced Computing Center (TACC) at The University of Texas at Austin for providing computing resources that have contributed to the research results reported within this paper.

■ REFERENCES

(1) Kumar, N. A.; Ganesan, V. *J. Chem. Phys.* **2012**, *136*, 101101.
(2) Thompson, B. C.; Fréchet, J. M. J. *Angew. Chem., Int. Ed.* **2008**, *47*, 58−77.
(3) Liu, F.; Gu, Y.; Jung, J. W.; Jo, W. H.; Russell, T. P. *J. Polym. Sci., Part B: Polym. Phys.* **2012**, *50*, 1018−1044.
(4) Bates, F. S.; Maurer, W. W.; Lipic, P. M.; Hillmyer, M. A.; Almdal, K.; Mortensen, K.; Fredrickson, G. H.; Lodge, T. P. *Phys. Rev. Lett.* **1997**, *79*, 849−852.
(5) Fredrickson, G. H.; Bates, F. S. *J. Polym. Sci., Part B: Polym. Phys.* **1997**, *35*, 2775−2786.
(6) Matsen, M. W. *J. Chem. Phys.* **1999**, *110*, 4658−4667.
(7) Hillmyer, M. A.; Maurer, W. W.; Lodge, T. P.; Bates, F. S.; Almdal, K. *J. Phys. Chem. B* **1999**, *103*, 4814−4824.
(8) Washburn, N. R.; Lodge, T. P.; Bates, F. S. *J. Phys. Chem. B* **2000**, *104*, 6987−6997.
(9) Düchs, D.; Ganesan, V.; Fredrickson, G. H.; Schmid, F. *Macromolecules* **2003**, *36*, 9237−9248.
(10) Huang, D. M.; Faller, R.; Do, K.; Moulé, A. J. *J. Chem. Theory Comput.* **2010**, *6*, 526−537.
(11) Lee, C.-K.; Pao, C.-W.; Chu, C.-W. *Energy Environ. Sci.* **2011**, *4*, 4124−4132.
(12) Kim, J. K.; Kimishima, K.; Hashimoto, T. *Macromolecules* **1993**, *26*, 125−136.
(13) Daoulas, K. C.; Müller, M. *J. Chem. Phys.* **2006**, *125*, 184904.
(14) Müller, M.; Smith, G. D. *J. Polym. Sci., Part B: Polym. Phys.* **2005**, *43*, 934−958.
(15) Edwards, E. W.; Müller, M.; Stoykovich, M. P.; Solak, H. H.; de Pablo, J. J.; Nealey, P. F. *Macromolecules* **2007**, *40*, 90−96.
(16) Pandav, G.; Ganesan, V. *Macromolecules* **2013**, *46*, 8334−8344.
(17) Pandav, G.; Ganesan, V. *J. Chem. Phys.* **2013**, *139*, 214905.
(18) Matsen, M. W.; Bates, F. S. *J. Chem. Phys.* **1997**, *106*, 2436−2448.
(19) Matsen, M. W.; Thompson, R. B. *J. Chem. Phys.* **1999**, *111*, 7139−7146.
(20) Fredrickson, G. *The Equilibrium Theory of Inhomogeneous Polymers*; Oxford University Press: New York, 2006.
(21) Olsen, B. D.; Shah, M.; Ganesan, V.; Segalman, R. A. *Macromolecules* **2008**, *41*, 6809−6817.
(22) Kipp, D.; Ganesan, V. *J. Phys. Chem. B* **2014**, *118*, 4425−4441.
(23) De Gennes, P. G.; Taupin, C. *J. Phys. Chem.* **1982**, *86*, 2294−2304.

DOI: 10.1021/acsmacrolett.5b00007
ACS Macro Lett. 2015, 4, 266−270